



ELSEVIER

Contents lists available at ScienceDirect

Computer Communications

journal homepage: www.elsevier.com/locate/comcom

Using barometric pressure data to recognize vertical displacement activities on smartphones

Salvatore Vanini*, Francesca Faraci, Alan Ferrari, Silvia Giordano

Information Systems and Networking Institute, Scuola Universitaria Professionale della Svizzera Italiana (SUPSI), via Cantonale, Manno, Switzerland

ARTICLE INFO

Article history:

Received 4 August 2014

Revised 19 February 2016

Accepted 20 February 2016

Available online xxx

Keywords:

Smartphone computing and communication

Activity recognition

Barometer

Sensor data

Inference model

Energy consumption

ABSTRACT

We introduce a novel, efficient methodology for the automatic recognition of major vertical displacements in human activities. It is based exclusively on barometric pressure measured by sensors commonly available on smartphones and tablets. We evaluate various algorithms to distinguish dynamic activities, identifying four different categories: standing/walking on the same floor, climbing stairs, riding an elevator and riding a cable-car. Activities are classified using standard deviation and slope of barometric pressure. We leverage three different inference models to predict the action performed by a user, namely: Bayesian networks, decision trees, and recurrent neural networks. We find that the best results are achieved with a recurrent neural network (reaching an overall error rate of less than 1%). We also show that decision tree classifiers can achieve good accuracy and offer a better trade-off between computational overhead and energy consumption; therefore, they are good candidates for smartphone implementations. As a proof of concept, we integrate the decision tree classifier in an App that infers user activity and measures elevation differences. Test results with various users show an average recognition accuracy rate of about 95%. We further show the power consumption of running barometric pressure measurements and analyse the correlation of pressure with environmental factors. Finally, we compare our approach to other standard methodologies for activity detection based on accelerometer and/or on GPS data. Our results show that our technique achieves similar accuracy while offering superior energy efficiency, independence from the sensor location, and immunity to environmental factors (e.g., weather conditions, air handlers).

© 2016 Published by Elsevier B.V.

1. Introduction

In the last decades, smartphones became the central computer and communication device in people's activities and lives. Current smartphones includes a variety of sensors that can be used for the continuous real-time location-aware monitoring of human activities as well as environmental conditions [1]. This has opened for research that ranged from very sensitive health applications [2] or privacy-concerned proximity solutions [3] up to leisure purposes [4]. Also, exploiting the multiplicity of mobile devices for large collection of measurements is beneficial to multiple fields, from health [5] to smart-cities [6]. Boosted up by smartphone computing and communication, activity recognition is spreading and developing: more and more applications rely on the knowledge of or on the distinction among human activities. Detecting the action a subject is performing can serve many purposes, for example, monitoring a variety of pathological conditions [7], or

17 sending alerts when a potentially dangerous activity is sensed [8],
18 or identifying lifestyle quality [9,10]. Collected information can be
19 valuable for suggesting countermeasures (e.g., stimulating physical
20 activity if a sedentary lifestyle is recognized). Other information,
21 as location, can be inferred (e.g., detecting floor transitions
22 when a subject passes from climbing stairs to standing still [11]). A
23 major challenge in designing an activity recognition system is the
24 user acceptance. If a system invades the private sphere, the user
25 might be reluctant to adopt it. With the rise of the smartphones,
26 a large part of the activity recognition research switched towards
27 wireless sensor measuring with mobile phones [12]. Smartphones
28 have the double advantage of both being equipped with multiple
29 sensors, and being an ubiquitous commercial product. Latest
30 generation of devices are indeed equipped with a rich set of sensors,
31 including accelerometer, barometric pressure sensor, compass,
32 gyroscope, proximity sensor, light sensor, GPS, microphone, and
33 camera. The key capabilities of sensing, computing and communicating
34 are integrated in the universally accepted and always-with-you
35 smartphone [1,13]. For these reasons, the detection of user activities
36 using sensors embedded in a smartphone is gaining a momentum.
37 Traditional methods for tracking activities with

* Corresponding author. Tel.: +41 586666586.

E-mail addresses: salvatore.vanini@supsi.ch (S. Vanini), francesca.faraci@supsi.ch (F. Faraci), alan.ferrari@supsi.ch (A. Ferrari), silvia.giordano@supsi.ch (S. Giordano).

38 smartphones mainly rely on integrated accelerometer sensors. 105
39 However, the difference in the way of performing a well defined 106
40 activity and of carrying the device, even for the same user, can 107
41 lead to a very poor accuracy [14]. A drawback of the accelerom- 108
42 eter sensor is energy consumption, which (if always on) is signif- 109
43 icant [15] and is mostly determined by the need of keeping the 110
44 phone's components active to access sensors results [16]. Emerg- 111
45 ing methodologies aim at applying multi-sensor data fusion tech- 112
46 niques, taking advantage of the abundance of sensors embedded 113
47 in smartphones and their complementarity [17,18]. Of course, the 114
48 use of multiple sensors negatively impacts energy consumption. At 115
49 present, the two major challenges in the accomplishment of good 116
50 activity detection with smartphones are still energy efficiency and 117
51 independence from the device's position along human body. In the 118
52 present work, we define a new class of activities - Vertical Dis- 119
53 placement Activities (VDAs) - where major movement is along the 120
54 vertical axis. Examples of VDAs can be standing, climbing stairs, 121
55 riding a cable-car, riding an elevator, or jumping. Our methodol- 122
56 ogy shows that it is possible to identify VDAs with very good ac- 123
57 curacy relying only on barometric pressure sensors available on 124
58 off the-shelf smartphones [11]. Barometric pressure sensors have 125
59 been traditionally used for height estimation by measuring pres- 126
60 sure changes [19]. Information derived from accelerometer data 127
61 and GPS based localization services can be integrated in a second 128
62 step, only if really needed. Pressure sensing can provide, for ex- 129
63 ample, complementary information to pedestrian dead reckoning. 130
64 The main advantage is that switching from a sensor to another 131
65 can extend battery life and optimize the detection analysis. More- 132
66 over pressure measurements are totally independent of the phone 133
67 position. 134

68 Our paper is structured as follows. We firstly discuss the liter- 135
69 ature (Section 2) and the rationale of our work (Section 3). In 136
70 Section 4 we present our experiments for investigating the char- 137
71 acteristics of barometric pressure in different scenarios. We de- 138
72 fined four different user dynamics mode ("standing/walking" on 139
73 the same floor, "climbing stairs", "riding a cable-car", and "riding 140
74 an elevator"). Then we collected training labelled data on baromet- 141
75 ric pressure in the corresponding scenarios. We tested three differ- 142
76 ent inference methods to classify trained data. The metric used to 143
77 choose the best model is a good trade-off between performance 144
78 and costs. It is widely known that recurrent neural networks are 145
79 the state of the art in inference models, however their implemen- 146
80 tation in resource-constrained devices (i.e. smartphones) presents 147
81 several issues due to their computational needs and their impact 148
82 on battery lifetime. On the other hand, decision trees and Bayesian 149
83 networks are less computationally demanding and have less im- 150
84 pact on energy consumption. The results presented in Section 5 151
85 show that, although the success rate of the Long Short-Term Mem- 152
86 ory [20] recurrent neural network to classify our barometric pres- 153
87 sure data was very high (only 0.9% of errors, on average), the J48 154
88 decision tree algorithm also had a very good performance, provid- 155
89 ing an average recognition rate of about 95%. For all these rea- 156
90 sons, J48 algorithm is the best choice for detecting VDAs on smart- 157
91 phones using barometric pressure data. We also directly mea- 158
92 sured battery consumption when sampling barometric pressure at 159
93 a constant rate and found that it is negligible. To demonstrate 160
94 the advantages of using pressure sensors for activity recognition 161
95 over sensors traditionally used (i.e., accelerometers and GPS), in 162
96 Section 6 we analyse and compare accuracy, energy efficiency, in- 163
97 door effectiveness and phone position independence. Finally, in 164
98 Section 7 – as a use case scenario – we describe an App for An- 165
99 droid where both barometer-based approaches to activity recogni- 166
100 tion and height estimation have been implemented. This App de- 167
101 tects user activity using the J48 decision tree algorithm and shows 168
102 the altitude graph, the current vertical speed and some statistics 169
103 about the activities performed by the user.

2. Related work

105 Many studies have focused on the identification of human 106
107 VDAs, such as standing, walking, climbing stairs and riding 108
109 up/down an elevator, from sensors data. 110

111 Several pieces of work have been performed with the analysis 112
113 of accelerometer data, as further discussed in Section 6.1. In gen- 114
115 eral, the accuracy of methods based on accelerometers depends on 116
117 the position of the sensors (or the phone that embeds sensors) 118
119 and accelerometers are energy-demanding. Kwapisz et al. [21] col- 120
121 lect data from a phone's accelerometer for 29 individuals. Data 122
123 is analysed and two patterns are identified (periodic and non- 124
125 periodic). Then, they use three classification techniques (decision 126
127 trees, logistic regression and multilayer neural networks) to pre- 128
129 dict the user activities. Krishnan and Panchanathan in [22] evaluate 130
131 the performance of different discriminative classifiers (i.e., Boosted 132
133 Decision Stumps, Support Vector Machines and Regularized Lo- 134
135 gistic Regression) to tackle continuous human activity recognition 136
137 based on accelerometer data. They propose to capture the rate at 138
139 which the acceleration changes for activities that have a signifi- 139
140 cant amount of motion (like walking, running, etc.), by comput- 140
141 ing statistical features like mean, variance and correlation on the 141
142 first order derivative of the acceleration data. The human-activity 142
143 recognition system proposed in [14] employs a smartphone with 143
144 a built-in triaxial accelerometer. It uses a combination of statisti- 144
145 cal signal features, artificial-neural nets and autoregressive mod- 145
146 elling to classify activities. The most cited paper about activity de- 146
147 tection using accelerometers is [23], where authors (Bao et al.) use 147
148 wearable accelerometers to classify a variety of every-day activi- 148
149 ties (including standing, climbing stairs and riding elevator). In [24] 149
150 barometric pressure data is used in combination with tri-axial ac- 150
151 celeration data and tri-axial gyroscope data to train classifiers and 151
152 recognize child activities. In [25] pressure sensors are used to im- 152
153 prove activity recognition based on acceleration data: in this case, 153
154 authors limit to plot measures of both barometric pressure and ac- 154
155 celeration, and to observe that the change in altitude connected to 155
156 a pressure change can help to provide a more sophisticated algo- 156
157 rithm for activity recognition, but they do not propose any algo- 157
158 rithm for activity detection. In [26] a dedicated multi-sensor board 158
159 containing seven different sensors (microphone, visible light pho- 159
160 totransistor, 3-axis accelerometer, 2-axis compass, barometer, am- 160
161 bient light, and humidity) is used to collect measurements from 160
162 twelve individuals, to infer a subject's activity and classify it as 161
163 sitting, standing, walking, walking up stairs, walking down stairs, 161
164 riding elevator down, riding elevator up, and brushing teeth. They 162
165 employ an ensemble of classifiers to select the most useful features 162
166 and then use those features to recognize the set of human move- 163
167 ments. A second layer of Hidden Markov Models (HMMs) combi- 163
168 nes the outputs of the classifiers to estimate the most likely ac- 164
169 tivity. Results show that three sensors yield the most discrimina- 164
170 tive information for recognizing activities: the audio, barometric 165
171 pressure and accelerometer sensors. This information is comple- 165
172 mentary: audio captures sounds produced during the various ac- 166
173 tivities, accelerometer data is sensitive to the movement of the 166
174 body, and barometric pressure helps detecting activities connected 167
175 to height variations, such as riding an elevator or moving up and 167
176 down stairs. In [27], four sensors (accelerometer, barometer, gyro- 168
177 scope and magnetometer) are employed to accurately recognize a 168
178 user's mode of motion when a height change is detected. The algo- 169
179 rithm developed has shown a good success rate (from 80 to 96%) 169
180 in discriminating among walking up or down stairs, riding an el- 170
181 evator, and standing or walking an escalator. In very few pieces 170
182 of work, GPS location data has been used to learn and recognize 171
183 the activities in which a person is engaged over a period. For ex- 171
184 ample, in [28] the authors extract a person's activities – such as 172
185 walking, driving a car, or riding a bus – from traces of GPS data, 172

169 using a probabilistic temporal model that is based on conditional
 170 Random fields (CRF) [29]. Similarly, in [30] generic activities typ-
 171 ically performed while a user stays at a location, such as work,
 172 leisure, sleep, visit, dining, are inferred from GPS data, using Re-
 173 lational Markov Networks. Such approaches suffer from low-level
 174 accuracy and flexibility. In [31], Sankaran et al. use only barometer
 175 to detect basic user activities such as *idle*, *walking* and *vehicle*. Their
 176 algorithm is based on the number and rate of altitude changes
 177 derived from the pressure measurements returned by barometric
 178 sensors. Our algorithm has a finer-granularity classification of dynamic
 179 modes as it can distinguish the transportation mode (i.e.,
 180 stairs, elevator or cable-car). Furthermore, the algorithm proposed
 181 by Sankaran et al. has a low detection accuracy of the walking
 182 mode, which forces them to fuse barometer and accelerometer
 183 to complement the barometer-based sensing. Using multiple sensors
 184 can help improving the detection of specific activities, especially
 185 when information from one sensor is insufficient to recognize
 186 them. However, a higher number of sensors involves high energy
 187 consumption and may increase the computational overhead. In [32]
 188 it is shown how pressure sensors data can be effectively used for
 189 floor localisation. The authors present an efficient indoor-stay
 190 recognition method requiring measurements such as vertical height
 191 between floors, current temperature, and atmospheric pressure
 192 value at a reference location, to accurately estimate the floor
 193 level. It is the only work where energy efficiency is considered, al-
 194 though it is not directly measured. There are also surveys about
 195 integrating sensors on garments for activity recognition tasks, but
 196 activities detected are more related to body postures and body-
 197 parts movements. For example, authors in [33] present a prototype
 198 using strain sensors to distinguish upper body postures. Authors
 199 in [34] use conductive textile based electrodes that can be easily
 200 integrated in garments to detect specific body activities (e.g., shak-
 201 ing head, looking down, speaking, looking left/right, etc.). Textiles
 202 have the same advantage of our approach: they have freedom in
 203 positioning of sensors. In addition, they provide space availability
 204 and are comfortable to wear. The main drawback of those studies
 205 is that they are still at a prototype and proof of concept stage. Us-
 206 ing sensors embedded in smartphones can be a better approach
 207 to activity recognition because smartphones are getting more and
 208 more common, they are likely to be with a user during his daily
 209 activities, have high processing power and adequate storage space,
 210 have relatively autonomy (before requiring a recharge), and are
 211 perceived as an unobtrusive device for most of the subjects.

212 To the best of our knowledge, there is no prior work that relies
 213 only on barometric pressure data coming from sensors embedded
 214 in smartphones for identifying individual's VDAs.

215 3. Rationale

216 Barometric pressure (or atmospheric pressure) is defined as the
 217 force per unit area exerted against a surface by the weight of the
 218 air above that surface. The standard unit for pressure is the pasc-
 219 al (Pa), which is equal to one Newton per square meter (N/m²).
 220 In meteorology, the hectopascal (hPa) unit is mainly used; 1 hPa
 221 corresponds to 100 Pa.

222 Pressure depends on altitude h and temperature. For altitudes
 223 below 11 Km, their relationship can be defined as

$$224 h = h_0 + (T_0/k) * ((P/P_0)^{-kR/gM} - 1) \quad (1)$$

224 where P_0 and T_0 are the pressure and temperature at sea level
 225 (1013.25 hPa and 288.15° K), R is the universal gas constant
 226 (8.31432 Nm/ Kmol), k is the lapse rate/drop in temperature with
 227 altitude (0.0065° K/m) valid from sea level to 11 km, g is the stan-

228 dard acceleration due to gravity constant (9.80665 m/s²), M is the
 229 molar mass of Earth's air (0.0289644 kg/mol) ¹.

The function in Eq. (1) is non-linear, but continuous and mono-
 230 tonically decreasing with pressure P . Several factors can influence
 231 barometric pressure: atmospheric events, temperature and hu-
 232 midity changes, air conditioning/ventilation systems, window/door
 233 opening.

234 Atmospheric events comprehend meteorological conditions:
 235 when the weather changes from cloud to sunny or to rainy, pres-
 236 sure changes significantly. A cold wind can influence a reading and
 237 cause an error of around 10 m in the derivation of the altitude.
 238 However this class of events has a larger time scale than the slid-
 239 ing window of the activities we want to classify. The typical time
 240 duration of human activities we would like to classify is from 5 to
 241 30 min, so sudden or slow changes in pressure due to modified
 242 weather conditions can be neglected.

243 Temperature changes can occur for example when a person ex-
 244 its from her/his warm office and enters a cold corridor and then
 245 goes outside a building; it can be shown that variations of 15°C
 246 result in an error of 14 cm in altitude estimation, while maximum
 247 error for a temperature span of 20°C is averagely of 20 cm in alti-
 248 tude estimation [35]. To compensate the error in pressure reading
 249 caused by sudden changes in temperature, current chips contain
 250 a temperature sensor bundled into the barometric sensor chipset.
 251 The driver reads both pressure as well as temperature, and com-
 252 pensates for the error in software. To verify the effects of temper-
 253 ature changes on pressure readings, we used a barometric pres-
 254 sure sensor enabled smartphone to measure pressure in a closed
 255 room of a building where an air conditioning system was operat-
 256 ing. We subsequently exited the room and measured pressure out-
 257 side. The results of the test showed that there were not any signif-
 258 icant changes in the values of barometric pressure. We repeated
 259 the same experiment in a closed room where a heating system
 260 maintained the temperature at 26°C (while the temperature out-
 261 side was 20°C). Also in this case, we didn't notice any significant
 262 pressure change.

263 When humidity changes, air density changes and therefore also
 264 pressure. However, when humidity increases from 50 to 90% the
 265 error introduced on altitude calculation is about 1 cm and there-
 266 fore negligible [35]. In [36], authors found that when an air han-
 267 dler was operating, barometric pressure in a living room raised by
 268 0.03 hPa. Similarly, a slight increase in air pressure of 0.015 hPa
 269 occurred in a master bedroom when its door was closed. Since
 270 these changes are below the relative pressure accuracy (0.1 hPa)
 271 of the sensors mounted in common smartphones, their impact on
 272 our measurements (and, indirectly, on our technique) is negligible.

273 If an application performs height estimation with barometric
 274 sensors, there is a need to constantly calibrate the values of base
 275 pressure and temperature, especially in outdoor conditions. This
 276 information is indeed provided by most airports and weather sta-
 277 tions. Indoor height estimation can be done quite precisely but
 278 only with a constant update of reference values as it is shown in
 279 [37]. As illustrated in the following sections, we will use differen-
 280 tial measurements to recognise activities, thus we can ignore refer-
 281 ence values.

282 In real-life situations, it is highly unlikely that external factors
 283 could mimic human activities and create artifacts. For example, to
 284 mimic stair climbing the temperature should decrease regularly at
 285 around 20°C per second, to mimic riding an elevator (speed ca. 1.5
 286 m/s) the opening of a door/window should bring an increase in
 287 pressure of 15–25 Pa per second. Furthermore, artifacts of small
 288 entity can be smoothed by using a proper smoothing algorithm as
 289

¹ International Organization for Standardization (ISO), Standard Atmosphere, ISO 2533:1975, 1975.

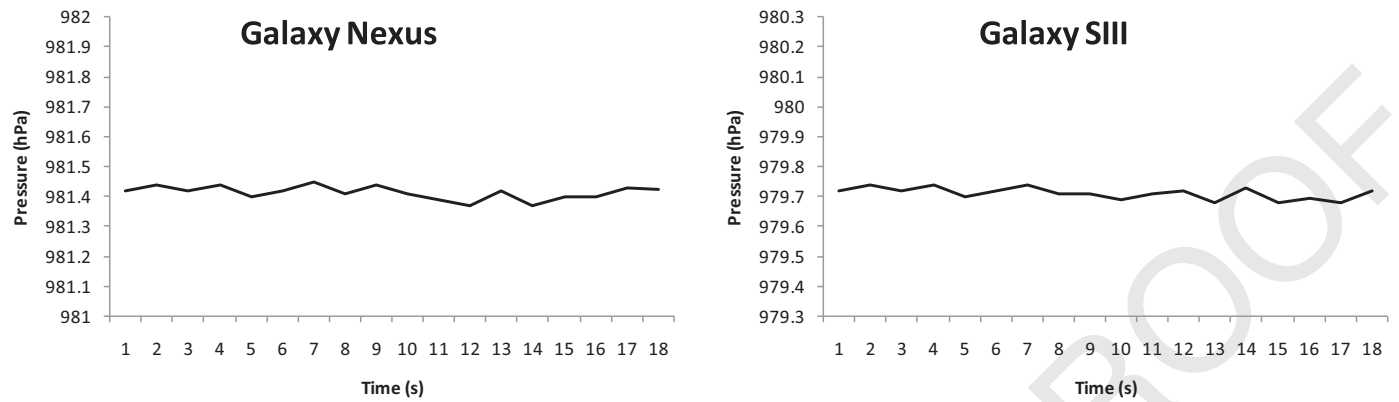


Fig. 1. Barometric pressure while a subject was standing still.

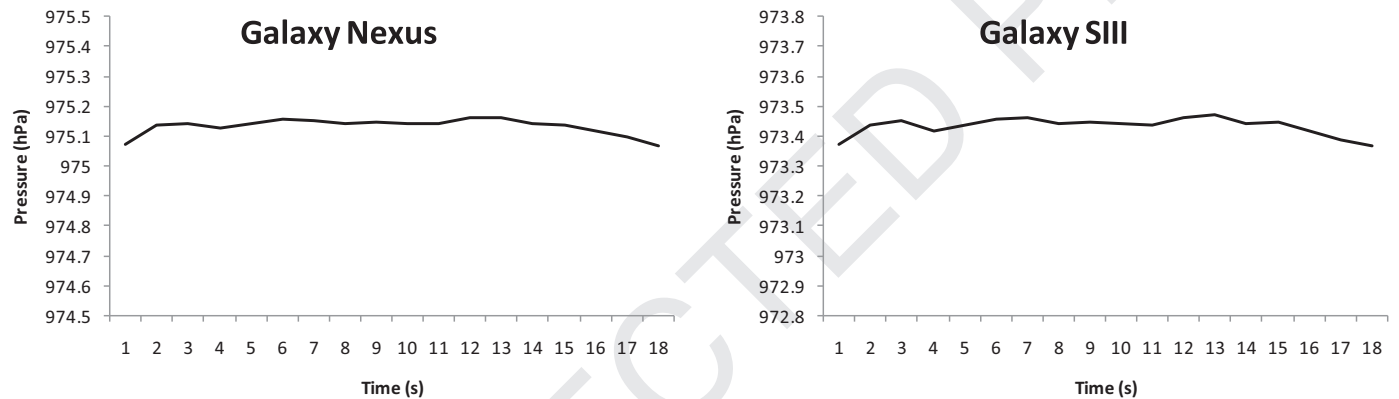


Fig. 2. Barometric pressure while a subject was walking on the same floor.

290 the one we used for our VDAs detection algorithm that is described
 291 in the following sections. In conclusion, Eq. (1) can be directly used
 292 for the present study without any modification.

293 4. System design

294 In this section, we describe the hardware (smartphones) used
 295 for our tests, the preliminary experiments we made to investigate
 296 the characteristics of barometric pressure in different scenarios, the
 297 process for collecting training data, and the method for deriving
 298 height information from pressure.

299 4.1. Hardware

300 To test the dynamics of pressure variations and check if they
 301 are the same for different sensors models, we conducted prelim-
 302 inary experiments using different mobile phones. For our tests,
 303 we used two Android v4 mobile phones models: Samsung Galaxy
 304 Nexus and Samsung Galaxy SIII. The first phone is equipped with a
 305 Bosch Sensortec BMP180 digital barometric pressure sensor, while
 306 the Samsung Galaxy SIII mounts a STMicroelectronics LPS331AP
 307 chip. Both sensors are based on piezo-resistive MEMS technology
 308 and have low power consumption (average current consumption
 309 in advanced mode is respectively, 30 and 32 μ A). The relative ac-
 310 curacy for pressure is ± 0.12 hPa for the BMP180 and ± 0.1 hPa for
 311 the LPS331AP chip.

312 4.2. Characteristics of barometric pressure

313 We first analysed the trend of raw pressure readings.

314 Android does not allow to set the sampling time for sensors
 315 data. We determined empirically that using the "SENSOR_DELAY_

FASTEST" rate for sensors events (0 μ s data delay) yields the best
 316 results. After each sensor read, we waited one second prior to the
 317 next read operation, thus emulating a sampling time of roughly
 318 1 Hz.
 319

320 To mitigate the residual noise, we applied the double exponen-
 321 tial smoothing method [38] to our time series because of its trend-
 322 tracking properties. If x_t is the raw data sequence of observations
 323 starting at time $t = 0$, s_t is used to represent the smoothed value
 324 at time t , and b_t is the best estimate of the trend at time t . Double
 325 Exponential Smoothing is given by:

$$\begin{aligned} s_t &= \alpha x_t + (1 - \alpha)(s_{t-1} + b_{t-1}) \\ b_t &= \gamma (s_t - s_{t-1}) + (1 - \gamma)b_{t-1} \end{aligned} \quad (2)$$

326 where α is the *data smoothing factor*, $0 \leq \alpha \leq 1$, and γ is the *trend*
 327 *smoothing factor*, $0 \leq \gamma \leq 1$. The initial values can be taken as $s_1 =$
 328 x_0 and $b_1 = x_1 - x_0$. The smoothing factor, for both the data and
 329 the corresponding trend, represents the importance applied to the
 330 most recent sample. We used 0.5 for both factors.

331 On other smartphone models (e.g., Nexus 5), the barometer
 332 chips performs smoothing internally, thus a smoothing technique
 333 in the code is not required [31].

334 To study the characteristics of pressure for the VDAs of differ-
 335 ent subjects, we recorded pressure in six different scenarios: while
 336 a subject was standing, while she was walking on the same floor
 337 of a building, while she was climbing and descending the stairs be-
 338 tween different floors of a building, while she was riding an eleva-
 339 tor from the bottom to the second floor of a building and, finally,
 340 while she was riding a cable-car. Results show that the pressure
 341 remains stable when a user is standing (Fig. 1) and is relatively
 342 stable when a user walks on the same floor (Fig. 2). When a sub-
 343 ject is climbing/descending stairs the pressure decreases/increases.

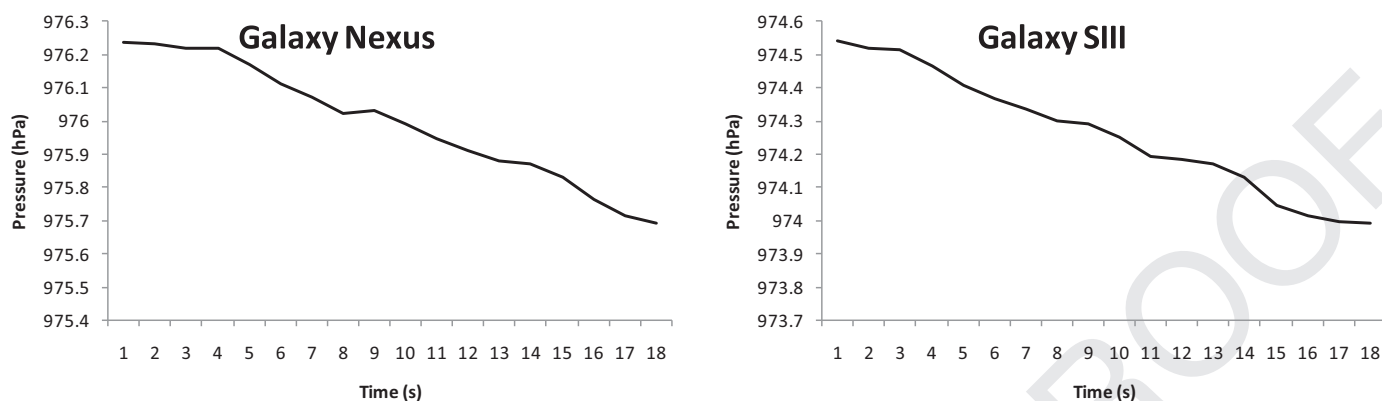


Fig. 3. Barometric pressure while a subject was climbing stairs.

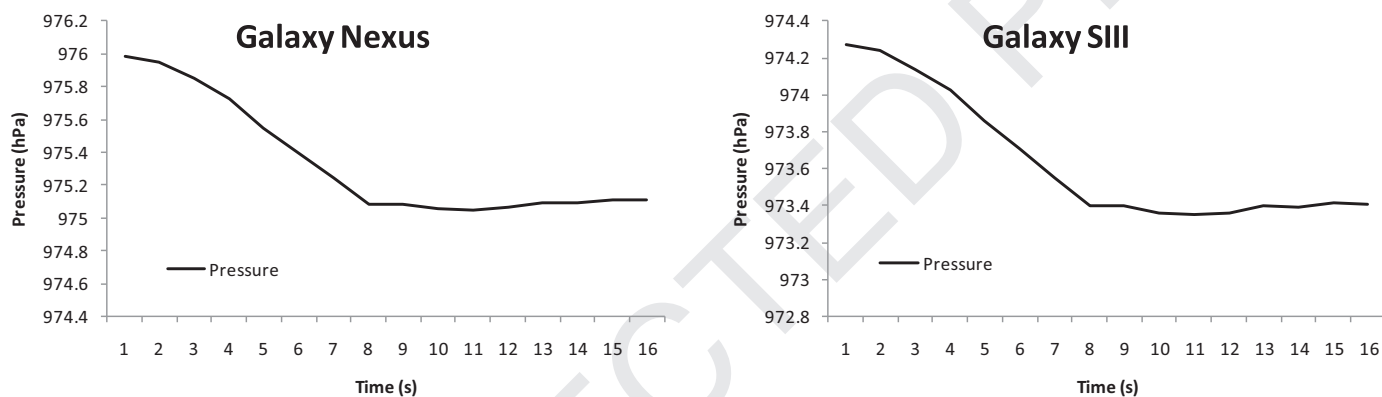


Fig. 4. Barometric pressure while a subject was riding an elevator up.

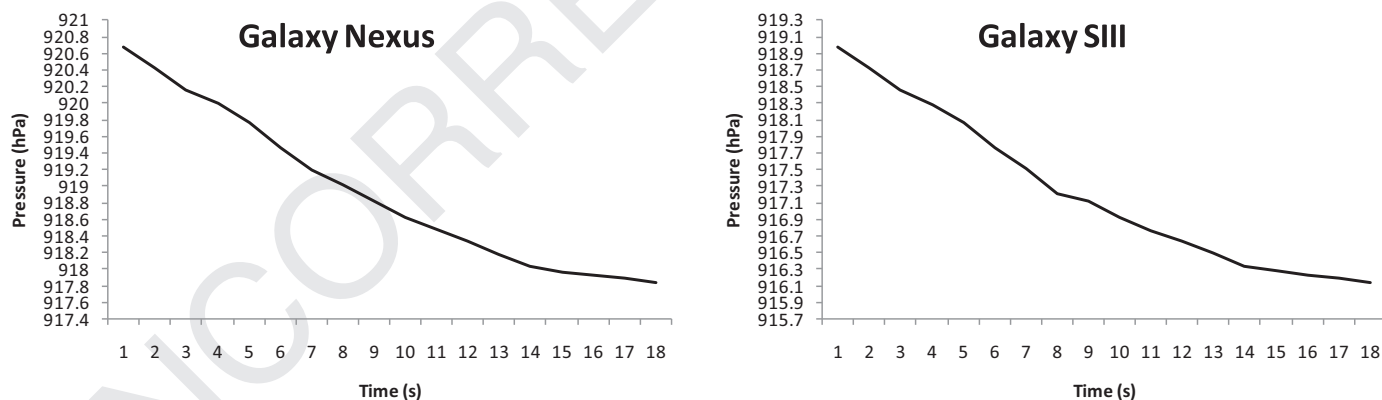


Fig. 5. Barometric pressure while a subject was riding a cable-car.

344 Fig. 3 shows the evolution of pressure while a subject was climbing
 345 stairs. When a subject is riding the elevator up, the pressure
 346 decreases at a higher rate than when climbing stairs, as illustrated
 347 in Fig. 4. Finally, when she rides a cable-car, barometric pressure
 348 varies significantly (Fig. 5). It can also be observed that the vertical
 349 speed of a user has the same dynamics – and can be easily
 350 inferred from the dynamics – of pressure variation over time. For
 351 example, the rate of pressure variation in elevators is higher, due
 352 to their higher rate of velocity.

353 The most important conclusion we derived from our set of exper-
 354 iments was that each VDA has distinct dynamics with regard
 355 to pressure variations. Furthermore, the standing and walking sce-
 356 narios exhibit the same behaviour in terms of pressure variation.
 357 Finally, although absolute values for pressure were different, dyn-
 358 amics were similar for both phones, thus the pressure variation

over time is independent of the type of sensor used for measuring 359
 it. 360

4.3. Training data collection 361

For our set of experiments in VDA recognition using barometric 362
 pressure data, we studied four types of activities: 363

- Standing/walking. 364
- Climbing stairs. 365
- Riding an elevator. 366
- Riding a cable-car. 367

The direction (up/down) while climbing stairs, riding an eleva- 368
 tor and riding a cable-car can be automatically inferred by com- 369
 puting the difference between the starting pressure and the end 370

pressure (the direction is “up” if the pressure decreases, “down” if it decreases)

To collect training data, we deployed an Android application that samples barometric pressure at a frequency of roughly 1 Hz (see Section 4.2). Subjects can label their activity by selecting the corresponding value from a spinner. Pressure values are recorded once a subject presses a *Start* button. Registration of pressure values is stopped after pressing a *Stop* button. Pressure data collected between the start and stop times are labelled with the name of the associated activities and stored in a SQLite database on the smartphone.

4.4. Feature computation

We performed features extraction on sliding windows with 50% overlap, which is fairly common in the literature [23,39,40]. We used a window of 8 samples (roughly 8 s). The features that we extracted from the sliding windows of barometric pressure were:

- Standard deviation.
- Slope: defined as the ratio between the change in barometric pressure over the window. This physical quantity gives an indication of how pressure varies over vertical displacement time.

5. Experiments and data analysis

We formulated activity detection as a classification problem, where classes are represented by labelled VDAs and test data instances are represented by the set of extracted features (standard deviation and slope) over barometric pressure measurements, collected using our Android application. We divided data sets into two different settings:

- Experiments with trained subjects (researchers).
- Experiments with untrained and unsupervised subjects.

We discriminated between the above two settings because the performance of classifiers may be significantly worse when applied on data collected by untrained persons, in real-world conditions. In the latter scenario, there are fewer constraints (e.g., subjects are not told exactly where and how to perform activities) with respect to a lab environment, where data is collected by scientists who perfectly know the behaviour of the phenomenon under observation. This observation has been remarked many times in related studies in literature. For example, [41] reported 95.8% activity recognition rates for data gathered in laboratory, but recognition rates dropped to 66.7% for data gathered outside the laboratory, in unconstrained settings.

Experiments were carried out by ten subjects: five from the academic community and five externals. Subjects performed their daily routines by recording and manually labelling actions corresponding to the four activities to detect, using our Android application. Training sets were acquired from the subjects themselves, in their workspaces, indoors and outdoors. On average, we gathered about 30 min of data per activity (around 1800 pressure readings per activity), per subject, except for the cable-car scenario, where traces were registered only by one trained and one untrained person, for about 15 min each. The phones we used for the experiments were the Samsung Galaxy Nexus and the Samsung Galaxy SIII. It is important to point out that experiments targeting the climbing stairs and riding elevator scenarios were performed in buildings with different layouts, without any prior knowledge of the building layout or any information about floor heights and about the number of steps between each floor (for the staircase scenario). In detail, floor height was in the range of (2.70; 3.40) m, while step height varied between 13 and 16 cm. Furthermore, experiments were run in different places, located at different elevations.

Table 1

Average values for features (standard deviation and slope) extracted from barometric pressure.

Activity	Std. Dev. (hPa)	Positive slope (hPa/s)	Negative slope (hPa/s)
Standing/Walking	0.00064	0.00456	-0.00438
Climbing stairs	0.006359	0.02671	-0.02961
Riding elevator	0.0828	0.1078	-0.0101
Riding cable-car	0.60346	0.2965	-0.29342

Table 2

Recognition accuracy for the activities studied with trained and untrained subjects for the J48 classifier.

Activity	Trained users (%)	Untrained users (%)
Standing/Walking	98.44	87.61
Climbing stairs	91.62	77.44
Riding elevator	95.14	88.25
Riding cable-car	99.99	99.99

Table 1 shows the average values for the features (standard deviation and slope) we extracted from the barometric pressure data, for the trained user scenario. We obtained similar results also for the untrained user scenario. As expected, the average value of the standard deviation for pressure increases as the amplitude of the vertical movement associated to the correspondent activity increases. The values for slope (i.e., the variation of pressure over time) confirm that pressure is almost stable when a subject is standing or walking, while it varies significantly when a subject is riding an elevator, and even more, when she/he is riding a cable-car. The dynamics for positive and negative variations are almost similar. Standard deviation and slope of pressure are correlated, since they both reflect a large amount of variation in the measurements of barometric pressure.

We split our analysis into two sections. In Section 5.1, we present machine learning algorithms, which are computationally cheap. A recurrent neural network algorithm – comparatively more computationally intensive – is instead presented in Section 5.2.

5.1. VDA detection with computationally cheap machine learning algorithms

We used the Weka Machine Learning Algorithm Toolkit [42] and evaluated the performance of two base-level classifiers: J48 Decision Trees and Naive Bayes. We found a quite significant difference between the trained and untrained scenario.

The highest recognition accuracy is reached by the J48 decision tree classifier. It was able to distinguish between the different activities with 95.06% average accuracy in the trained scenario and 83.20% average accuracy in the untrained scenario. In the trained scenario, 1.56% of the standing/walking instances were incorrectly classified as climbing stairs, while 5.13% instances of the climbing stairs scenario were wrongly detected as standing/walking and 3.25% as riding elevator. Finally, 4.86% instances of the riding elevator scenario were incorrectly detected as climbing stairs. Table 4 summarizes the aforementioned results. We found a similar behaviour also for the untrained scenario, but for the standing/walking case, where traces collected by untrained individuals were also classified as riding elevator (Table 5). Table 2 shows the results of activities recognition for the J48 classifier, while Table 3 shows the performance results for the Naive Bayes classifier. As it can be noticed, classification accuracy for the riding cable-car scenario is almost 100% in both cases: this is not surprising because this scenario has the lowest relative standard deviation of the training data (0.2 for standard deviation and 0.11 for slope).

Table 3

Recognition accuracy for the activities studied with trained and untrained subjects for the Naive Bayes classifier.

Activity	Trained users (%)	Untrained users (%)
Standing/Walking	94.91	90.38
Climbing stairs	88.78	68.1
Riding elevator	90.67	73.6
Riding cable-car	99.99	99.99

Table 4

Distribution of incorrectly classified activities for trained subjects with the J48 classifier.

Activity	Standing/Walking	Climbing stairs	Riding elevator	Riding cable-car
Standing/Walking	–	1.56%	0%	0%
Climbing stairs	5.13%	–	3.25%	0%
Riding elevator	0%	4.86	–	0%
Riding cable-car	0%	0%	0%	–

Table 5

Distribution of incorrectly classified activities for untrained subjects with the J48 classifier.

Activity	Standing/Walking	Climbing stairs	Riding elevator	Riding cable-car
Standing/Walking	–	11.49%	0.89%	0%
Climbing stairs	20.50%	–	1.57%	0%
Riding elevator	0%	11.75	–	0%
Riding cable-car	0%	0%	0%	–

475 The main reason the J48 classifier has better performance than
 476 the Naive Bayes classifier is that Naive Bayes makes use of all the
 477 features extracted, and analyses them individually as though they
 478 are equally important and independent of each other. This is not
 479 our case, because standard deviation and absolute value of the
 480 pressure slope are correlated (as explained in Section 5).

481 5.2. VDA detection with a recurrent neural network

482 To show the effectiveness of our barometric pressure-based
 483 approach, we tested a recurrent neural network to learn and
 484 classify our pressure time series composed of long time lags of
 485 unknown size between different activities. We used the PyBrain²
 486 machine learning library to implement a Long Short-Term Memory
 487 (LSTM) neural network. We chose LSTM because the activities to
 488 discriminate are repetitive (e.g., if a subject is climbing stairs at
 489 time t , it is highly likely that she will still be climbing stairs at
 490 time $t + 1$) and they can be modelled with a recurrent network.
 491 Furthermore, LSTM outperforms other recurrent networks in many
 492 areas (e.g., regular, context-free and context sensitive languages
 493 [43]; handwriting recognition [44]; discriminative keyword spot-
 494 ting [45]). Another key factor is that LSTM can handle very large
 495 time lags, say of the order of several hundreds or thousands [46].

496 As any recurrent neural network, LSTM uses feedback connec-
 497 tions to store representations of recent inputs events. In addition, it
 498 contains blocks that automatically determine when an input is sig-
 499 nificant enough to be stored. For training, we used the Rprop [47]
 500 supervised learning technique, which is an adaptive gradient based
 501 technique (computation of the gradient of an error measurement
 502 in weight space) known for its high convergence speed, accuracy
 503 and robustness.

504 With regard to the network architecture, we used 2 input units
 505 (standard deviation and slope) and 1 output unit (activity to be de-

Table 6

Average test error rates with trained subjects for the LSTM neural network.

Activity	Test error rate(%)
Standing/Walking	1.29
Climbing stairs	0.22
Riding elevator	1.47
Riding cable-car	1.01

506 tected). For LSTM, we used 5 hidden units, an output layer with a
 507 softmax function (because we are doing classification), and a re-
 508 current connection from the hidden to the hidden layer that looks
 509 one timestamp back in time. The input layer has connections to
 510 all units in the hidden layer. The output layer received connections
 511 only from the hidden layer. Since we used the Rprop trainer, all
 512 training samples have the same weight.

5.2.1. Results

513 We extrapolated 1500 samples from the set of measurements
 514 collected by the five trained users. The resulting training set was
 515 randomly split into 60% training and 40% test data sets. We initially
 516 ran some training iterations to set the values of the Rprop param-
 517 eters that provided the minimum test error. After those tests, we
 518 decided to use 0.4 for *etaminus* (factor by which step width is de-
 519 creased when overstepping) and 4 for *deltamax* (maximum step
 520 width). Then, we ran 50 training iterations, each of which stopped
 521 after the training module converged.

522 The LSTM algorithm nearly always learns to solve the VDA
 523 recognition task. The best test set error was only 0.22%. On av-
 524 erage, the training module converged after 120 epochs. Table 6
 525 shows the details of the test error rates for each activity.
 526

5.3. Weather dependence

527 To demonstrate that our VDA detection algorithm is inde-
 528 pendent of changing weather conditions, we collected 24 h of
 529 traces with different weather conditions. We started from scattered
 530 clouds to variable clouds with isolated rain showers. The phone
 531 was lying still in the same position and we checked if changes in
 532 the barometric pressure under such variable weather conditions
 533 could trigger false positives and be detected as either climbing
 534 stairs, or riding an elevator or riding a cable-car.
 535

536 The accuracy of the standing/walking mode was found to be
 537 99.45%, showing that weather changes do not impact on the capa-
 538 bility of our algorithm to detect VDAs. This is because weather drift
 539 occurs over a larger time scale than the temporal duration of our
 540 VDAs. Furthermore, rather than having frequent ups and downs as-
 541 sociated with rapid pressure changes, weather drift is usually in
 542 one direction, and gradual.

543 Fig. 6 shows the pressure variation during a day due to changes
 544 of atmospheric events for a phone laying in the same position,
 545 along with the indication of the VDA detected. As it can be seen
 546 from the picture, the pressure trend follows weather changes. Fur-
 547 thermore, false positives (lighter lines in the picture) were trig-
 548 gered only relatively to the climbing stairs scenario.

5.4. Power consumption

549 We measured the power needed to retrieve barometric pres-
 550 sure values. Measurements were made at two different levels of
 551 granularity.

552 First, we implemented an App for monitoring significant
 553 changes in the battery level – specifically when a device enters
 554 a low battery state. The App can also be configured for reading
 555

² <http://www.pybrain.org>

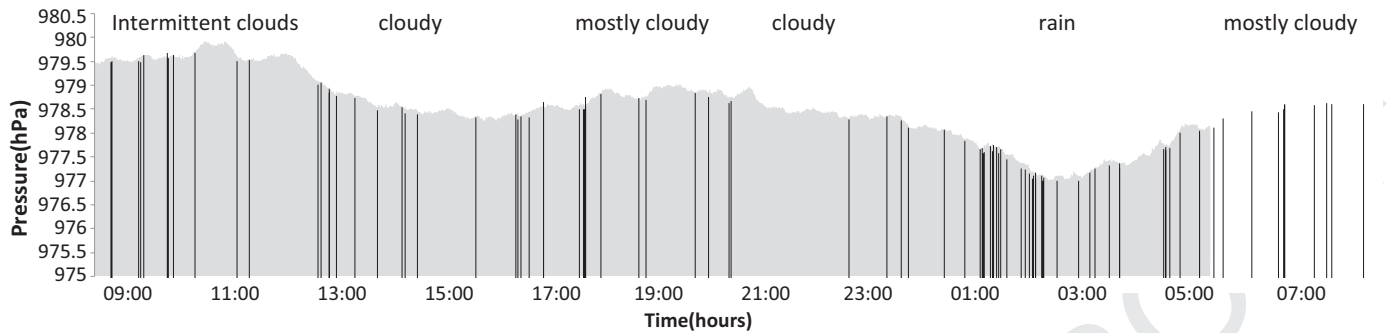


Fig. 6. Evolution of barometric pressure in a day along with the indication of false positives (darker lines) in the detected activity, while a phone was standing still.

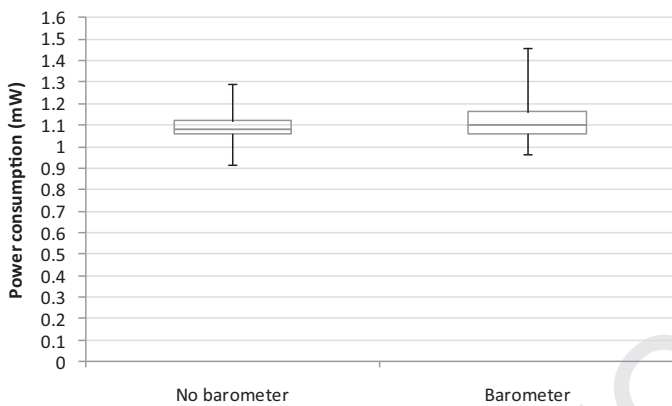


Fig. 7. Power consumption without and with (1 Hz) pressure readings.

line with the current consumption ($30\mu\text{A}$) of the pressure sensor specified in the technical data sheet. In fact, since voltage supply required by the smartphone is 3.7 V, the power needed to read barometric pressure is about 0.12 mW. The remaining amount (0.01 mW) is due to the OS. It is important to emphasize that power consumption did not change when we moved (vertically) the device (which is the gesture that allows to discriminate about the different activities).

6. Comparison with other sensors and methodologies

As described in Section 2, the current approaches to VDA recognition using sensors are mainly based on accelerometers and GPS sensors. In the following sections, we compare the performance of our VDA detection based on pressure sensors with such approaches in terms of accuracy, energy efficiency, indoor effectiveness and phone position independence.

6.1. Accelerometer-based approaches

We start our comparison analysis with accelerometers. In terms of accuracy, Bao et al. [23] obtain the best performance results with decision tree classifiers, getting an accuracy rate of 95.67% for standing still, but recognition rates were significantly lower when riding elevators and climbing stairs (respectively 43.58 and 85.61%). Lester et al. [26] achieved their best result for climbing stairs, where the classification was correct 95% of the time. The accuracy for descending stairs and riding elevator up/down was respectively 89%, 87.3% and 84.6%. Authors were also able to recognize walking and standing activities, but in the latter accuracy was very low (55%). Results obtained by Kwapisz et al. in [21] show that the accuracy of recognizing the standing activity was up to 93.3%, while climbing stairs was inferred with about 60% accuracy at best. Krishnan et al. [22] show that Boosted Decision Stumps (Adaboost) classifiers have the best performance, achieving about 90% recognition accuracy for walking, standing, and climbing stairs scenarios. Khan et al. in [14] claim a 99% accuracy rate for the detection of sitting, 95% accuracy for walking and climbing stairs, and 92% accuracy for descending stairs.

Fig. 9 offers an overview of the accuracy rates in recognizing VDAs for the methods described above and our method (in the best case of trained users). Accuracy rates obtained with our barometric-based approach are in line with – and in some case better than – the numbers reported above.

With regard to energy efficiency, to get comparable data, we implemented an App that measures the acceleration force (in m/s^2) applied to a smartphone on all three physical axes (x , y , and z) and monitored the power consumption with our POEM tool. The App listens to accelerometer sensor events at a sampling rate of approximately 1Hz (as in the case of the App for reading

barometric pressure data at a sample rate of approximately 1 Hz. It keeps the screen on at full brightness.

We started from a full-charged device, stopped all applications and services, run our application and measured the time until a low battery state was detected with pressure readings and without pressure readings. It took respectively 5.21 and 5.7 h to reach the low battery state, thus showing an overall impact well below 10%.

To get a more accurate measure of the power (in mW) needed to read values from pressure sensors, we employed a portable open sourced power monitor (POEM) [48] – similar to BattOr [49] – using the open source hardware platform Arduino³. To synchronize the external board with the smartphone, we used LED2LED communication [50] between a LED mounted on the Arduino board and the camera on the smartphone. POEM offers mW accuracy and a sampling rate down to ms for measuring power consumption.

Fig. 7 shows the boxplots of power consumption for two different scenarios: idle mode and pressure readings at a sample rate of approximately 1Hz. As it can be seen from the picture, the increase of power consumption due to the sampling of barometric pressure is negligible: the value of the second quartile for the “pressure reading” scenario is indeed slightly higher than the corresponding value in the “no pressure reading” scenario. The variability of power consumption is higher in the “pressure reading” scenario, where it can reach at most about 1.5 mW. This means that the power required to read pressure data is not always constant (this could be due to the OS). The average value of energy consumed by the smartphone when the App was reading pressure values from the barometric sensor was 1.23 mW, while it was 1.1 mW when the App was in idle state. Therefore, energy required for reading pressure values was about 0.13 mW on average. This value is in

³ <http://www.arduino.cc>

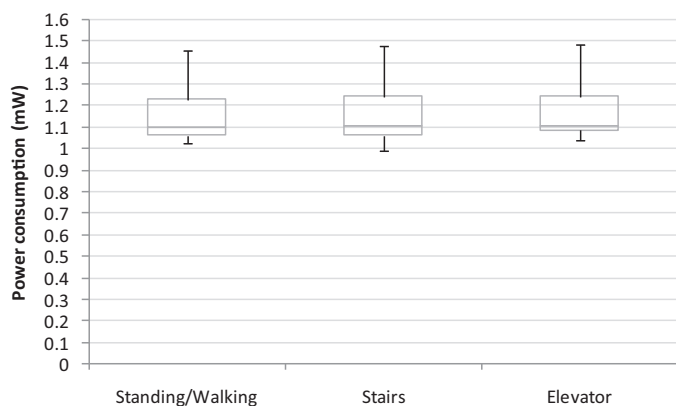


Fig. 8. Power consumption for reading acceleration data.

pressure data). We reproduced three of the four VDAs types studied in the paper. We omitted the cable-car scenario because accelerations related to this use-case are not easy to reproduce as they are very high. For example, during our set of experiments in VDA recognition, we measured an average acceleration of 2.6 m/s^2 . Fig. 8 shows the boxplots of power needed for reading acceleration data in a temporal window of 10 s, in each of the three scenarios considered. We measured the power consumption at a sample rate of 100 ms. From the plots, it can be seen that the variability of the power consumption is almost the same in all three scenarios, but it is in any case higher than in the “no pressure reading” scenario described in Section 5.4. The power required to measure acceleration was overall the same in all three cases, so it does not depend on the intensity of the movement. On average, the power consumed by the App when reading acceleration data was about 1.37 mW: this means that energy required to read data from the acceleration sensor is about 0.27 mW.

The accuracy of activity recognition based on accelerometer data depends on the position of the sensors (or phone) and their orientation [14,26,51–53]. Conversely, during our experiments in VDA detection, we intentionally failed to control the position of the phone, as it happens in a daily usage pattern. We found that under this realistic conditions, the accuracy of VDA detection was unaffected by changes in the phone’s on-body location (in pockets, hands, or even bags) and orientation of the phone. This finding is one of the main strengths of barometer pressure-based activity recognition and is also one of the key differences from accelerometer-based activity detection.

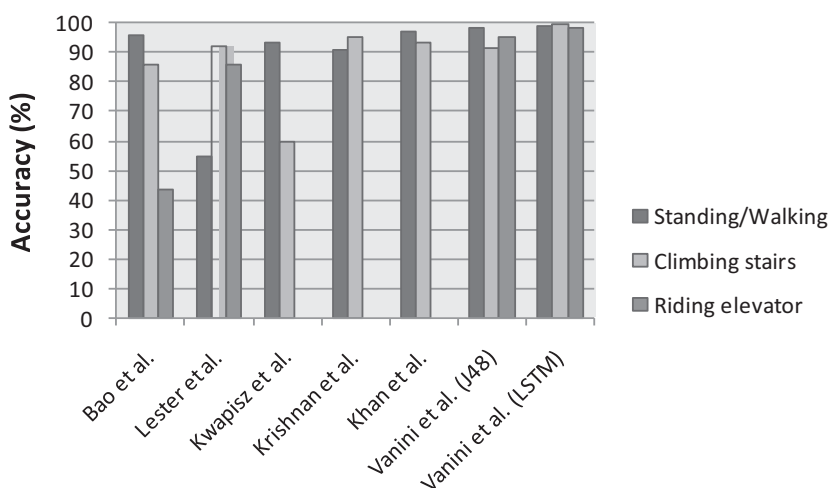


Fig. 9. Comparison of accuracy rates for inferring VDAs with accelerometers.

Table 7

Average power consumption in GPS receiver chips on smartphones.

Manufacturer	CSR	u-blox	MediaTek	Sony
Model	SirfSTAR IV GSD4t	Max-7 u-blox 7	MT3333	CXD5600GF
Continuous tracking (1 Hz)	40 mW	50 mW	19 mW	10 mW
Cyclic tracking (1 Hz)	8 mW	13.5 mW	N.A.	N.A.

6.2. GPS-based approaches

We have also compared barometers and GPS sensors in terms of activity recognition accuracy, height estimation, power consumption and sensor-position independence.

As already described in Section 2, methods based on GPS data for activity detection have low-level accuracy and flexibility.

Compared to GPS positioning, the main advantage of a pressure-based approach to vertical displacement measurement is that, as widely reported in literature, the accuracy of the barometer height estimation exceeds that of GPS. Furthermore, barometer is not subject to shadowing as GPS (which also impacts on the accuracy and availability of the altitude measurement), thus it can be used in an indoor environment.

In terms of power consumption, it is well-known that smartphone battery usage increases a lot when GPS interface is on [54]. Table 7 lists the average power consumption claimed by the most popular manufacturers (CSR, u-blox, MediaTek, Sony corp) of GPS receiver chips for smartphones. The table distinguishes among continuous tracking and cyclic tracking modes. In the first mode, the receiver continuously tracks all the available satellites to achieve the best possible position accuracy. In cyclic tracking, the receiver employs intermittent tracking to conserve power: a significant amount of power is saved by periodically turning off the Radio Frequency (RF) front-end and most of the hardware in this mode. From the table, it can be seen that even the lowest values for power consumption are higher than the average power (0.13 mW) consumed by the pressure sensor.

Finally, since the GPS accuracy is very low, the position of the phone does not have a significant impact on activity detection.

Table 8 recaps the features compared in our analysis for the three sensors, using star ratings (out of a maximum of 3 stars). It can be noticed that GPS is the only sensor that is not working indoor, thus it cannot be used neither for activity detection nor for

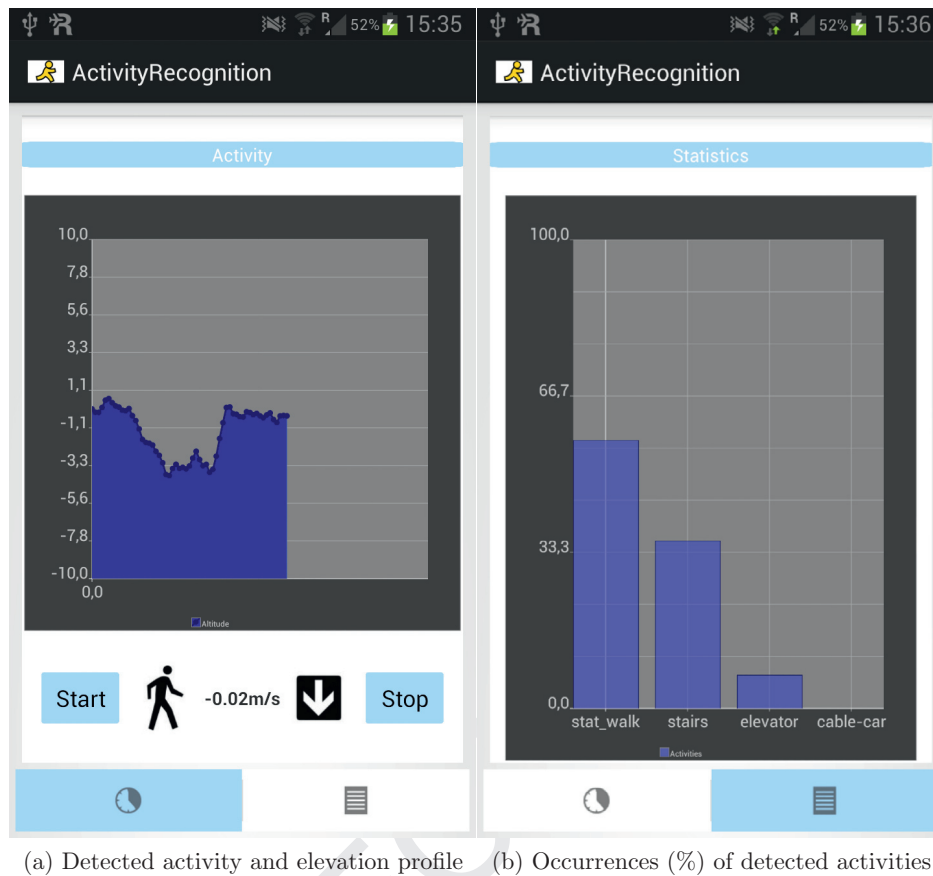


Fig. 10. GUI of the App implementing activity recognition.

Table 8

Comparison of sensors for VDA detection on a 3 star bases.

Sensor	Detection accuracy	Energy efficiency	Indoor effectiveness	Position independence
Accelerometer	***	**	***	*
GPS	*	*	N.A.	**
Barometer	***	***	***	***

altitude estimation in that scenario. Barometer is the only sensor that has a 3 star rating for all the metrics analysed.

To summarize, the performance of our proposed pressure-based method is comparable and in most cases better than the performance of traditional systems based on acceleration data, but it has the significant advantage of being energy-efficient.

7. Use case scenario: an application for detecting user activities and measuring altitude differences

As a use case scenario, we implemented an App for Android to infer the VDAs carried out by a user and to show statistics about them.

We used the Weka library for Android⁴ and utilized a training set of instances that we collected during our experiments. Although LSTM has better accuracy, its power consumption is significant, as reported in [55]. To comply with energetic constraints, we chose the J48 decision tree classifier. In fact, J48 provides very good accuracy results and has a linear complexity for both training and inferencing activities, resulting in a small impact on energy consumption.

⁴ <https://github.com/rjmarsan/Weka-for-Android>

The App also estimates and shows the elevation profile during a user's journey. This is done by converting the pressure measured by the barometer to elevation information, using a simplified version of Eq. (1). As it can be seen from that equation, absolute height information cannot be calculated without the proper knowledge of local sea level pressure, which varies depending on weather conditions. Reference barometer information can be obtained via an auxiliary TCP/IP server connection, which is not always available. Furthermore, a high level of accuracy for altitude is not required. For these reasons, we can use a simplified version of Eq. (1). Assuming constant weather conditions and that the typical air pressure at the sea level is 1013 hPa, it can be easily derived that near the Earth's surface a difference of 1hPa corresponds approximately to 8.4 m in elevation.

Finally, the information about elevation changes is also used to derive the vertical speed of a user.

This use case scenario shows the potential of pressure sensors and the large number of application fields where pressure sensors can be employed.

Fig. 10 shows the user interface of the App, which is composed of two tabs. The home tab contains two buttons for starting and stopping activity detection. Elevation changes are shown in a graph, while current activity and direction are shown as an icon. Vertical speed (in m/s) is displayed at the centre of the screen. The second tab contains a graph that shows statistics about the activities performed during a start-stop session and their occurrences.

8. Conclusion

The barometer is one of the least frequently used sensors on smartphones, but is also one of the most promising. In this work, we demonstrated the advantages of the use of barometric pressure

data from sensors embedded in mobile phones to recognize vertical displacement activities. We evaluated the performance of three different models to infer user activities and found that the LSTM recurrent neural network has a very high accuracy rate. However, J48 decision tree algorithm is a good choice for resource-constrained devices owing to its fairly high accuracy, its low computational overhead, and (consequently) its low energy consumption. We implemented an Android application that integrates the J48 decision tree algorithm and infers the activity performed by a user. The application uses barometric pressure data to provide information on the vertical distance travelled by a user and also shows it instantaneously on a graph. We also showed that barometric pressure sensors have many advantages over sensors traditionally used for activity recognition (namely, accelerometers and GPS) in terms of accuracy, energy efficiency, indoor effectiveness and independence from the phone position. The use of barometric data for activity recognition is very advantageous, as many applications that cannot be correctly recognized with accelerometer can be easily inferred with pressure data. Furthermore, the barometric sensor can enhance the quality of accelerometer sampling whenever a vertical displacement is present but is not the main movement. Finally, the barometer can also be used as a trigger to accelerometer sensing when the barometer itself cannot achieve a sufficient quality, resulting in a more power-efficient approach.

Future work includes the use of multiple sensors for activity detection and the implementation of a mechanism for switching between sensors – and their underlying methodology – depending on geo-position, predominant activity, and objective functions like e.g., battery life and accuracy optimization.

References

- [1] S. Giordano, D. Puccinelli, When sensing goes pervasive, *Pervasive Mobile Comput.* 17 (2015) 175–183.
- [2] A. Puiatti, S. Mudda, S. Giordano, O. Mayora, Smartphone-centred wearable sensors network for monitoring patients with bipolar disorder, in: Proceedings of the 2011 Annual International Conference of the IEEE Engineering in Medicine and Biology Society, EMBC, IEEE, 2011, pp. 3644–3647.
- [3] P. Kotzanikolaou, C. Patsakis, E. Magkos, M. Korakakis, Lightweight private proximity testing for geospatial social networks, *Comput. Commun.* 73 (2016) 263–270.
- [4] E. Miluzzo, M. Papandrea, N.D. Lane, A.M. Sarroff, S. Giordano, A.T. Campbell, Tapping into the vibe of the city using vibn, a continuous sensing application for smartphones, in: Proceedings of 1st International Symposium on From Digital Footprints to Social and Community Intelligence, ACM, 2011, pp. 13–18.
- [5] Z. Yu, Y. Liang, B. Guo, X. Zhou, H. Ni, Facilitating medication adherence in elderly care using ubiquitous sensors and mobile social networks, *Comput. Commun.* 65 (2015) 1–9.
- [6] F. Theoleyre, T. Watteyne, G. Bianchi, G. Tuna, V.C. Gungor, A.-C. Pang, Networking and communications for smart cities special issue editorial, *Comput. Commun.* 58 (2015) 1–3.
- [7] C.N. Scanaill, S. Carew, P. Barralon, N. Noury, D. Lyons, G.M. Lyons, A review of approaches to mobility telemonitoring of the elderly in their living environment, *Ann. Biomed. Eng.* 34 (4) (2006) 547–563.
- [8] L. Panini, R. Cucchiara, A machine learning approach for human posture detection in domestic applications, in: Proceedings of the 12th International Conference on Image Analysis and Processing, 2003, IEEE, 2003, pp. 103–108.
- [9] M. Papandrea, M. Zignani, S. Gaito, S. Giordano Cremonese, G.P. Rossi, How Many Places Around You? (2013).
- [10] M. Zignani, M. Papandrea, S. Gaito, S. Giordano, G.P. Rossi, On the key features in human mobility: relevance, time and distance, in: Proceedings of 2014 IEEE International Conference on Pervasive Computing and Communications Workshops (PERCOM Workshops), IEEE, 2014, pp. 260–265.
- [11] S. Vanini, S. Giordano, Adaptive context-agnostic floor transition detection on smart mobile devices, in: Proceedings of 2013 IEEE International Conference on Pervasive Computing and Communications Workshops (PERCOM Workshops), IEEE, 2013, pp. 2–7.
- [12] M. Conti, C. Boldrini, S.S. Kanhere, E. Mingozzi, E. Pagani, P.M. Ruiz, M. Younis, From manet to people-centric networking: milestones and open research challenges, *Comput. Commun.* 71 (2015) 1–21.
- [13] S. Giordano, D. Puccinelli, The human element as the key enabler of pervasiveness, in: Proceedings of 2011 the 10th IFIP Annual Mediterranean Ad Hoc Networking Workshop (Med-Hoc-Net), IEEE, 2011, pp. 150–156.
- [14] A.M. Khan, Y.-K. Lee, S. Lee, T.-S. Kim, Human activity recognition via an accelerometer-enabled-smartphone using kernel discriminant analysis, in: Proceedings of 2010 5th International Conference on Future Information Technology (FutureTech), IEEE, 2010, pp. 1–6.
- [15] Y. Man, E.C.-H. Ngai, Energy-efficient automatic location-triggered applications on smartphones, *Comput. Commun.* 50 (2014) 29–40.
- [16] B. Priyantha, D. Lymberopoulos, J. Liu, Litterlock: enabling energy-efficient continuous sensing on mobile phones, *Pervasive Comput. IEEE* 10 (2) (2011) 12–15.
- [17] R.K. Ganti, S. Srinivasan, A. Gacic, Multisensor fusion in smartphones for lifestyle monitoring, in: Proceedings of 2010 International Conference on Body Sensor Networks (BSN), IEEE, 2010, pp. 36–43.
- [18] A.M. Khan, A. Tufail, A.M. Khattak, T.H. Laine, Activity recognition on smartphones via sensor-fusion and kda-based svms, *Int. J. Distrib. Sens. Netw.* 2014 (2014).
- [19] G. Liu, M. Iwai, Y. Tobe, D. Matekenya, K.M.A. Hossain, M. Ito, K. Sezaki, Beyond horizontal location context: measuring elevation using smartphone's barometer, in: Proceedings of the 2014 ACM International Joint Conference on Pervasive and Ubiquitous Computing: Adjunct Publication, ACM, 2014, pp. 459–468.
- [20] S. Hochreiter, J. Schmidhuber, Long short-term memory, *Neural Comput.* 9 (8) (1997) 1735–1780.
- [21] J.R. Kwapisz, G.M. Weiss, S.A. Moore, Activity recognition using cell phone accelerometers, *ACM SigKDD Explor. Newslett.* 12 (2) (2011) 74–82.
- [22] N.C. Krishnan, S. Panchanathan, Analysis of low resolution accelerometer data for continuous human activity recognition, in: Proceedings of IEEE International Conference on Acoustics, Speech and Signal Processing, 2008. ICASSP 2008, IEEE, 2008, pp. 3337–3340.
- [23] L. Bao, S.S. Intille, Activity recognition from user-annotated acceleration data, in: *Pervasive Computing*, Springer, 2004, pp. 1–17.
- [24] S. Boughorbel, J. Breebaart, F. Bruekers, I. Flinsenbergh, W. ten Kate, Child-activity recognition from multi-sensor data, in: Proceedings of the 7th International Conference on Methods and Techniques in Behavioral Research, ACM, 2010, p. 38.
- [25] A. El Halabi, H. Artail, Integrating pressure and accelerometer sensing for improved activity recognition on smartphones, in: Proceedings of 2013 Third International Conference on Communications and Information Technology (IC-CIT), IEEE, 2013, pp. 121–125.
- [26] J. Lester, T. Choudhury, G. Borriello, A practical approach to recognizing physical activities, in: *Pervasive Computing*, Springer, 2006, pp. 1–16.
- [27] M. Elhoushi, J. Georgy, A. Wahdan, M. Korenberg, A. Noureldin, Using portable device sensors to recognize height changing modes of motion, in: Proceedings of 2014 IEEE International Instrumentation and Measurement Technology Conference (I2MTC), IEEE, 2014, pp. 477–481.
- [28] L. Liao, D. Fox, H. Kautz, Hierarchical conditional random fields for GPS-based activity recognition, in: *Robotics Research*, Springer, 2007, pp. 487–506.
- [29] J. Lafferty, A. McCallum, F.C. Pereira, Conditional random fields: Probabilistic models for segmenting and labeling sequence data (2001).
- [30] L. Liao, D. Fox, H. Kautz, Blocation-based activity recognition using relational Markov networks, in: Proceedings of 19th International Joint Conference on Artificial Intelligence, Edinburgh, Scotland, 2005, pp. 773–778.
- [31] K. Sankaran, M. Zhu, X.F. Guo, A.L. Ananda, M.C. Chan, L.-S. Peh, Using mobile phone barometer for low-power transportation context detection, in: Proceedings of the 12th ACM Conference on Embedded Network Sensor Systems, ACM, 2014, pp. 191–205.
- [32] K. Komeda, M. Mochizuki, N. Nishiko, User activity recognition method based on atmospheric pressure sensing, in: Proceedings of the 2014 ACM International Joint Conference on Pervasive and Ubiquitous Computing: Adjunct Publication, ACM, 2014, pp. 737–746.
- [33] C. Mattmann, O. Amft, H. Harms, G. Tröster, F. Clemens, Recognizing upper body postures using textile strain sensors, in: Proceedings of the 11th IEEE International Symposium on Wearable Computers, 2007, IEEE, 2007, pp. 29–36.
- [34] J. Cheng, O. Amft, P. Lukowicz, Active capacitive sensing: exploring a new wearable sensing modality for activity recognition, in: *Pervasive Computing*, Springer, 2010, pp. 319–336.
- [35] C. Bollmeyer, T. Esemann, H. Gehring, H. Hellbruck, Precise indoor altitude estimation based on differential barometric sensing for wireless medical applications, in: Proceedings of 2013 IEEE International Conference on Body Sensor Networks (BSN), IEEE, 2013, pp. 1–6.
- [36] J. Lstiburek, K. Pressnail, J. Timusk, Air pressure and building envelopes, *J. Build. Phys.* 26 (1) (2002) 53–91.
- [37] B. Li, B. Harvey, T. Gallagher, Using barometers to determine the height for indoor positioning, in: Proceedings of the 2013 International Conference on Indoor Positioning and Indoor Navigation (IPIN), IEEE, 2013, pp. 1–7.
- [38] C. Croarkin, P. Tobias, Nist/sematech e-handbook of statistical methods, NIST/SEMATECH (2006). July. Available online: <http://www.itl.nist.gov/div898/handbook>
- [39] R.W. DeVaul, S. Dunn, Real-time motion classification for wearable computing applications (2001). 2001 Project Paper.
- [40] K. Van Laerhoven, O. Cakmakci, What shall we teach our pants? in: Proceedings of the Fourth International Symposium on Wearable Computers, IEEE, 2000, pp. 77–83.
- [41] F. Foerster, M. Smeja, J. Fahrenberg, Detection of posture and motion by accelerometry: a validation study in ambulatory monitoring, *Comput. Human Behav.* 15 (5) (1999) 571–583.
- [42] I.H. Witten, E. Frank, *Data Mining: Practical Machine Learning Tools and Techniques*, Morgan Kaufmann, 2005.
- [43] F.A. Gers, J. Schmidhuber, Lstm recurrent networks learn simple context-free and context-sensitive languages, *IEEE Trans. Neural Netw.* 12 (6) (2001) 1333–1340.

- 903 [44] A. Graves, J. Schmidhuber, Offline handwriting recognition with multidimen- 923
904 sional recurrent neural networks, in: *Advances in Neural Information Process-* 924
905 *ing Systems*, 2009, pp. 545–552. 925
- 906 [45] S. Fernández, A. Graves, J. Schmidhuber, An application of recurrent neural net- 926
907 works to discriminative keyword spotting, in: *Proceedings of Artificial Neural* 927
908 *Networks–ICANN 2007*, Springer, 2007, pp. 220–229. 928
- 909 [46] A.F. Atiya, A.G. Parlos, New results on recurrent network training: unifying 929
910 the algorithms and accelerating convergence, *IEEE Trans. Neural Netw.* 11 (3) 930
911 (2000) 697–709. 931
- 912 [47] C. Igel, M. Hüsken, Improving the rprop learning algorithm, in: *Proceedings of* 932
913 *the Second International ICSC Symposium on Neural Computation (NC 2000)*, 933
914 2000, Citeseer, 2000, pp. 115–121. 934
- 915 [48] A. Ferrari, D. Gallucci, D. Puccinelli, S. Giordano, Detecting energy leaks in an- 935
916 droid app with poem, in: *Proceedings of 2015 IEEE International Conference* 936
917 *on Pervasive Computing and Communication Workshops (PerCom Workshops)*, 937
918 IEEE, 2015, pp. 421–426. 938
- 919 [49] A. Schulman, T. Schmid, P. Dutta, N. Spring, Demo: phone power monitoring 939
920 with batter, in: *Proceedings of the 17th ACM International Conference on Mo-* 940
921 *bile Computing and Networking, MobiCom*, vol. 11, Citeseer, 2011. 941
- [50] S. Schmid, G. Corbellini, S. Mangold, T.R. Gross, An led-to-led visible light com- 923
munication system with software-based synchronization, in: *Proceedings of* 924
2012 IEEE Globecom Workshops (GC Wkshps), IEEE, 2012, pp. 1264–1268. 925
- [51] L. Sun, D. Zhang, B. Li, B. Guo, S. Li, Activity recognition on an accelerometer 926
embedded mobile phone with varying positions and orientations, in: *Ubiqui-* 927
tous Intelligence and Computing, Springer, 2010, pp. 548–562. 928
- [52] U. Maurer, A. Smailagic, D.P. Siewiorek, M. Deisher, Activity recognition and 929
monitoring using multiple sensors on different body positions, in: *Proceed-* 930
ings of International Workshop on Wearable and Implantable Body Sensor Net- 931
works, 2006. BSN 2006, IEEE, 2006, pp. 4–pp. 932
- [53] L. Atallah, B. Lo, R. King, G.-Z. Yang, Sensor placement for activity detection us- 933
ing wearable accelerometers, in: *Proceedings of 2010 International Conference* 934
on Body Sensor Networks, IEEE, 2010, pp. 24–29. 935
- [54] Y. Qi, C. Yu, Y.-J. Suh, S.Y. Jang, Gps tethering for energy conservation 1, in: 936
Proceedings of 2015 IEEE Wireless Communications and Networking Confer- 937
ence (WCNC), IEEE, 2015, pp. 1320–1325. 938
- [55] A. Ferrari, D. Puccinelli, S. Giordano, Gesture-based soft authentication, in: *Pro-* 939
ceedings of 2015 IEEE 11th International Conference on Wireless and Mobile 940
Computing, Networking and Communications (WiMob), IEEE, 2015, pp. 771– 941
777.